



Why Is Uranyl Formohydroxamate Red?

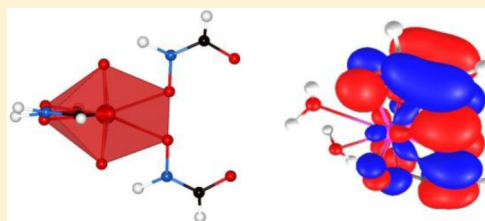
Mark A. Silver,[†] Walter L. Dorfner,[‡] Samantha K. Cary,[†] Justin N. Cross,[†] Jian Lin,[†] Eric J. Schelter,^{*,‡} and Thomas E. Albrecht-Schmitt^{*,†}

[†]Department of Chemistry and Biochemistry, Florida State University, 102 Varsity Way, Tallahassee, Florida 32306, United States

[‡]P. Roy and Diana T. Vagelos Laboratories, Department of Chemistry, University of Pennsylvania, 231 South 34th Street, Philadelphia, Pennsylvania 19104, United States

Supporting Information

ABSTRACT: The complexation of UO_2^{2+} by formohydroxamate (FHA^-) creates solutions with dark red coloration. The inherent redox activity of formohydroxamate leads to the possibility that these solutions contain U(V) complexes, which are often red. We demonstrate that the reaction of U(VI) with formohydroxamate does not result in reduction, but rather in formation of the putative *cis*-aquo $\text{UO}_2(\text{FHA})_2(\text{H}_2\text{O})_2$, whose polymeric solid-state structure, $\text{UO}_2(\text{FHA})_2$, contains an unusually bent UO_2^{2+} unit and a highly distorted coordination environment around a U(VI) cation in general. The bending of the uranyl cation results from unusually strong π donation from the FHA^- ligands into the $6d$ and $5f$ orbitals of the U(VI) cation. The alteration of the bonding in the uranyl unit drastically changes its electronic and vibrational features.



Hydroxamate complexes of U(VI) have been documented for many decades and, in fact, play several practical roles in uranium chemistry. Among these is the use of hydroxamates tethered to polymers to extract uranium from seawater where vast stores of uranium exist.¹ However, the foremost application of hydroxamates in actinide chemistry comes from their use as reductants for higher oxidation states of neptunium and plutonium in industrial uranium extraction processes.² This method relies on the resistance of U(VI) to reduction by the hydroxamate, whereas both Np(VI) and Pu(IV) are reduced to lower oxidation states. These conditions enable subsequent biphasic extractions based on the differences in the hydrophobicity of the actinide complexes in solution. Acetohydroxamate is typically used in this process, but recent work suggests that the simplest hydroxamate, the formohydroxamate anion (FHA^-) in Figure 1, may be preferable.³

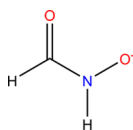


Figure 1. Structure of formohydroxamate anion.

A number of investigators have reported that the complexation of U(VI) by FHA^- leads to the formation of a red complex.⁴ We found this coloration perplexing because it is atypical of U(VI), which, in the absence of a chromophore, is typically yellow in solution. We speculated that the origin of the red color could be due to reduction to U(V). UO_2^+ complexes containing a formally U(V) ion, while uncommon, are known to have a red coloration.⁵ We have probed this chemistry to find that our original supposition is incorrect, and that the

answer is far more interesting. The unusual coloration of $\text{UO}_2(\text{FHA})_2$ results from distortions of the coordination geometry of U(VI) that include bending of the uranyl cation's O–U–O angle. These distortions result from the unusually strong donor capabilities of the formohydroxamate anion.

We repeated the standard preparation of $\text{UO}_2(\text{FHA})_2$ by reacting an aqueous solution of uranyl nitrate with FHA^- in a 1:2 metal-to-ligand ratio. As observed by May et al. the reaction mixture changed from a yellow-green color to red-orange upon addition of FHA^- .⁵ The absorption spectrum of this solution matches those already reported.⁵ The solution was set undisturbed for 7 days to slowly evaporate, yielding red crystals of $\text{UO}_2(\text{FHA})_2$.

Single crystal X-ray diffraction studies reveal a chain structure for $\text{UO}_2(\text{FHA})_2$ as shown in Figure 2. The fundamental building unit is a $\text{UO}_2(\text{FHA})_2$ molecule assembled from a uranyl cation that is chelated by two FHA^- anions. The molecule possesses 2-fold symmetry. However, the oxygen atoms of the N–O moieties of the FHA^- anions serve as μ_2 -oxo atoms in that they bridge between two uranyl cations thereby creating the chains. Similar chain formation is observed in the structure of $\text{UO}_2(\text{IO}_3)_2$.⁶

An examination of the angular distortions in the $\text{UO}_2(\text{FHA})_2$ unit reveals that it is atypical in a number of regards. The coordination environment around uranium is a UO_8 unit. However, it is distorted significantly from the classical hexagonal bipyramidal geometry with six oxygen atom donors at positions orthogonal to a linear UO_2^{2+} cation. There are two notable features of the distorted unit. First, the UO_2^{2+} cation is

Received: February 3, 2015

Published: May 9, 2015

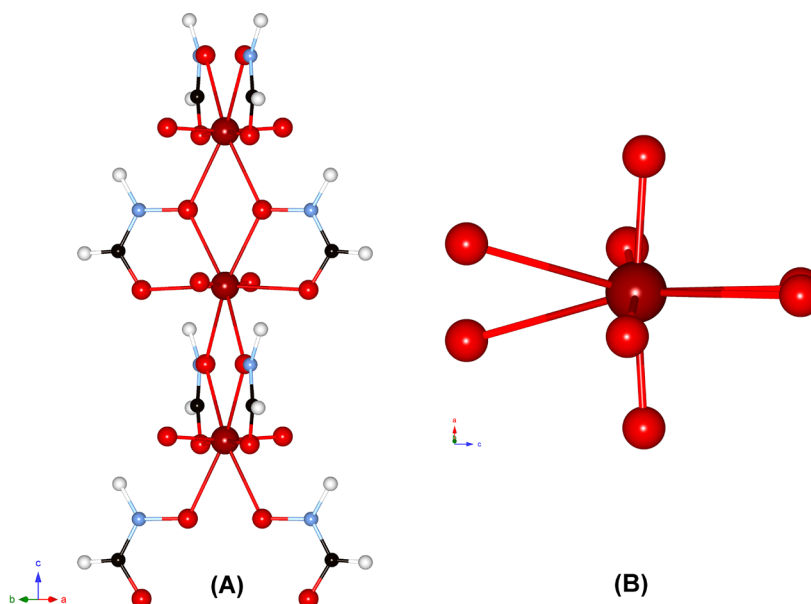


Figure 2. (A) Depiction of the helical chains that result from the bridging of the $\text{UO}_2(\text{FHA})_2$ units by μ_2 -oxo atoms of the N–O moiety. (B) View of the $\text{UO}_2(\text{FHA})_2$ unit showing the highly distorted UO_8 coordination environment.

fairly bent with an O–U–O angle of $173.5(4)^\circ$. While uranyl units are often not perfectly linear, these distortions seldom exceed 2° , and are typically caused by secondary contacts to the terminal oxo atoms. Even so the bend does not approach the 6.5° observed here. Notable exceptions to this include $\text{UO}_2(\text{O}-2,6\text{-}^t\text{Bu}_2\text{C}_6\text{H}_3)_2(\text{THF})_2\cdot\text{THF}$, $\text{UO}_2(\text{SCS})(\text{py})_2$, $\text{UO}_2(\text{BIPM}^{\text{TMS}})(\text{DMAP})_2$, and $\text{UO}_2(\text{Np-CAO-H}_2)(\text{NO}_3)(\text{CH}_3\text{OH})$.⁷ In the last example, the Np-CAO- H_2 amidoxime ligand has an electronic structure similar to that of the FHA ligand reported here. The uranyl compound was isolated as red crystals, and the O–U–O bond angle was reported to be $177.1(3)^\circ$. We offer that the causes of the red coloration in these compounds may be related. While the bending in $\text{UO}_2(\text{FHA})_2$ does not achieve the geometry of the long sought *cis*-uranyl cation, it may improve our understanding of how to access such a species.^{7–9} Second, the angular distortions of the six donor atoms comprising the FHA^- anions are significant. These would normally be expected to be both coplanar and orthogonal to the uranyl cation. While the four oxygen atoms from the two chelating FHA^- anions are approximately coplanar, the two additional donors from the μ_2 -oxo atoms are twisted by 46° with respect to the four oxygen atoms from the chelating ligands. The bend of the uranyl cation is directed away from the μ_2 -oxo ligands, and the angle between an oxygen atom of the uranyl unit and a μ_2 -oxo ligand is 110° . The twist within the equatorial plane yields a helical chain as the molecules propagate along the *c* axis.

Despite the large angular distortions, the bond distances within the UO_8 unit are quite normal. Foremost is the $\text{U}\equiv\text{O}$ bond distance of $1.779(6)$ Å ($\times 2$). This distance is expected for a U(VI) ,¹⁰ UO_2^{2+} cation, and is smaller than that for typical U(V) complexes.¹¹ The equatorial distances are also typical of a U(VI) complex and range from $2.447(6)$ to $2.504(6)$ Å.

Absorption and photoluminescence data were collected from solutions and single crystals of $\text{UO}_2(\text{FHA})_2$. There are changes in the absorption spectra upon crystallization as shown in Figure 3, although the visual color remains the same as that of the solutions (*vide infra*). It should be noted that the compound crystallizes in an orthorhombic space group; there

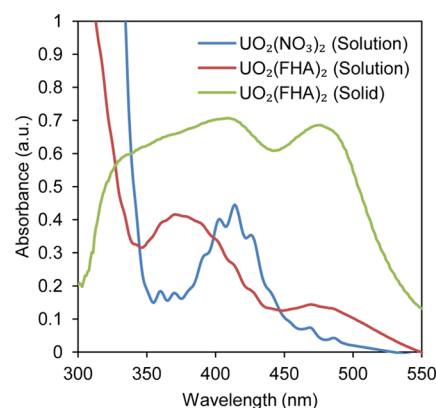


Figure 3. Solution and solid-state absorbance spectra of $\text{UO}_2(\text{NO}_3)_2$ and $\text{UO}_2(\text{FHA})_2$.

is necessarily an orientational dependence for the solid-state electronic spectra derived from single crystals (i.e., pleochroism), and the intensities of the transitions cannot be directly compared between solutions and the solid state.¹² We propose that these changes likely arise from dehydration of the putative solution species *cis*-aquo $\text{UO}_2(\text{FHA})_2(\text{H}_2\text{O})_2$, where, upon crystallization, the water molecules are displaced by the μ_2 -oxo atoms of bridging N–O moieties. It may be that such effects have not been noted before because extended X-ray fine structure data are two-dimensional and do not provide bond angle information, and the bond distances are exactly what would be expected for a typical U(VI) complex. In the computational study that follows, we have replaced the μ_2 -oxo ligand from the bridging N–O groups with water molecules to represent the solution structure. Upon optimization, we obtained a geometry comparable to that found in the polymeric crystal structure, which supports our choice of model complex.

The geometry for model complex $\text{UO}_2(\text{FHA})_2(\text{H}_2\text{O})_2$ (1) was optimized using the B3LYP hybrid DFT method with the 6-31G* basis set on H, N, O, and C atoms. The ECP60MWB core potential was applied to uranium.¹³ A conductor-like polarizable continuum model solvent model was used in all

optimization and frequency calculations to represent the dielectric of solvation by water.¹⁴ The results of the optimization of **1** show a U=O bond distance of 1.786 Å and an O—U—O angle of 173.6°. Both of these metrics are in good agreement with the experimental values of 1.779(6) Å and 173.5(4)°, respectively. The computational package NBO6 was used to detail contributions to the bonding of $\text{UO}_2(\text{FHA})_2(\text{H}_2\text{O})_2$.¹⁵ The U—ON bond comprises 8.0% U and 92.0% O atomic orbital contributions, suggesting a primarily ionic interaction. The contribution from the oxygen atom is approximately sp^2 (36.5% *s* and 63.5% *p*), and the contribution from uranium is primarily composed of 47.7% *5f* and 34.1% *6d* orbitals.

The Mayer bond order (MBO) determined for the U—ON bond of $\text{UO}_2(\text{FHA})_2(\text{H}_2\text{O})_2$ is 0.57, and the average MBO for the U=O bonds is 2.13.¹⁶ The natural charge on the uranium is +1.84, and the charges on the uranyl oxygen atoms are −0.65. When a related uranyl nitrate complex, $\text{UO}_2(\text{NO}_3)_2(\text{H}_2\text{O})_2$ (**2**), is computationally evaluated through an identical DFT treatment, we observe a uranium natural charge that is slightly higher at +1.87 and uranyl oxygen atoms with a slightly less negative natural charge of −0.60. The U=O bond order of **2** also increases slightly to 2.16. These changes suggest that the uranyl fragment of $\text{UO}_2(\text{FHA})_2(\text{H}_2\text{O})_2$ has a distorted electronic structure compared to that of **2**.

We sought to further investigate how the FHA^- ligand was destabilizing the uranyl bonding and causing the deviation from linearity of the O=U=O fragment observed in the crystal structure and optimized structure. The O—U—O bond angle was determined to be 178.4° for **2** compared to 173.6° for **1**. The difference highlights the effect of the equatorial ligand environment through a bending of almost 5° from exchange of the equatorial NO_3^- ligands with FHA^- . The computed U=O bond distances for the nitrate complex were 1.768 Å, which were 0.018 Å shorter than those in the optimized FHA^- complex.

Another method for evaluating destabilization of the uranyl bonding fragment is examination of the uranyl *trans*–*cis* isomerization free energy. One of us and others have used this approach previously to compare the relative stabilities of high-valent uranium bis-imido and uranyl complexes.¹⁷ For the current case, we computed the total free energy of the *cis*-uranyl form of $\text{UO}_2(\text{FHA})_2(\text{H}_2\text{O})_2$ (*cis*-**1**), whose O—U—O angle was optimized from an initial guess of 90°, and compared it to the total free energy of the *trans*-uranyl form of **1**. The O—U—O angle of *cis*-**1** did not require restriction and converged at a value of 97.69°. The same comparison was made for the uranyl nitrate complexes **2** and *cis*-**2**. The O—U—O angle required restriction at 97.69° in the computation for *cis*-**2** to match the O—U—O angle in *cis*-**1**. This locking was required to prevent rearrangement to the *trans*-uranyl that occurred during optimization of *cis*-**2**. The results, summarized in Figure 4, show that the *trans*–*cis* isomerization was +32.5 kcal mol^{−1} uphill for the nitrate complex, but only +17.9 kcal mol^{−1} uphill for the FHA^- complex. The 14.6 kcal mol^{−1} difference in the free energy for this reaction suggests that the FHA^- ligand may destabilize the *trans*-uranyl and/or stabilize the resulting *cis*-uranyl complexes. Due to steric encumbrance at the uranium ion in *cis*- $\text{UO}_2(\text{FHA})_2(\text{H}_2\text{O})_2$, a water molecule was liberated to the secondary coordination sphere during its optimization. Two complexes, *cis*-**1'** and *cis*-**2'**, were calculated as *cis*-uranyl complexes with one water molecule fully removed to better represent this structural change. The energies of those reactions

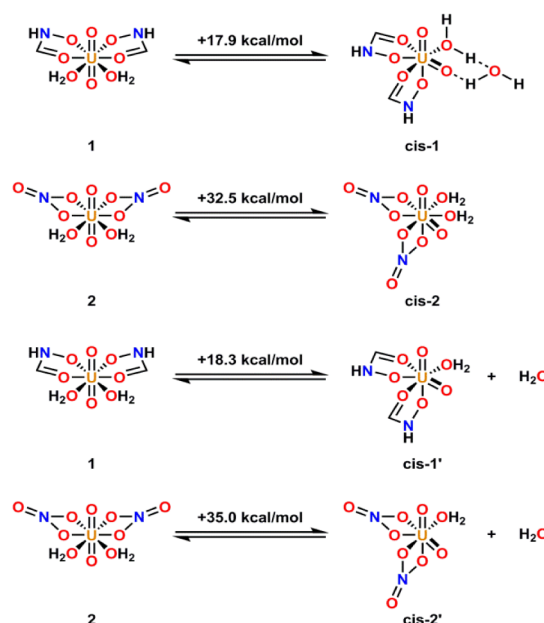


Figure 4. DFT calculated *cis*–*trans* isomerization free energies of the uranyl formohydroxamate model complex and a related uranyl nitrate model.

were found to be 18.3 and 35.0 kcal mol^{−1}, respectively, resulting in an even larger difference in ΔG of 16.7 kcal mol^{−1} between the dehydrated *cis* and *trans* forms.

The absorption spectra for the FHA^- complexes are shown in Figure 2, and are compared with that of $\text{UO}_2(\text{NO}_3)_2 \cdot 6\text{H}_2\text{O}$. Uranyl compounds typically absorb near 420 nm owing to ligand-to-metal charge transfer (LMCT), and this band usually displays well-defined vibronic progressions as displayed by $\text{UO}_2(\text{NO}_3)_2 \cdot 6\text{H}_2\text{O}$. Uranyl compounds also normally emit green light with a λ_{max} near 520 nm when irradiated with UV light.¹⁸ This photoluminescence is also strongly vibronically coupled. In the solution spectrum of $\text{UO}_2(\text{FHA})_2$, the LMCT feature normally found at 420 nm is hypsochromically shifted by ~50 nm, and a new band is found at 475 nm; the latter is not present in classical uranyl compounds. This feature is responsible for the red color because all of the short visible wavelengths are absorbed by $\text{UO}_2(\text{FHA})_2$. The FHA^- uranyl complex is also not luminescent in the solid state. In short, the electronic structure has been dramatically altered from what is typically observed in uranyl compounds.

Vibrational spectroscopy is also informative in the analysis of uranyl compounds with an intense asymmetric stretch often observed near 900 cm^{−1} and a symmetric stretch near 870 cm^{−1}. Raman and IR spectra were obtained from single crystals and are provided in the Supporting Information (Figures S1 and S2). An intense feature is observed in the Raman and IR spectra of $\text{UO}_2(\text{FHA})_2$ at about 827 cm^{−1} that likely corresponds to the ν_1 stretch of the uranyl cation. This stretch is assigned using the DFT frequency calculations. Its significant shift is suggestive of weakening of the U=O bonds, similar to the weakening of the O—U—O bond in the activated compound [(py)₃LiOUO(py)Li(py)(HL)], whose asymmetric stretch is reported at 708 cm^{−1}.¹⁹ In $\text{UO}_2(\text{FHA})_2$, C—N and N—O bands of the ligand are found at 1044 and 1236 cm^{−1}, respectively.

DFT computed IR and Raman spectra are shown to match well with the experimental spectra following application of a

scaling factor of 0.9613 for basis set correction (Supporting Information Figures S1 and S2).²⁰ The solution electronic absorption spectrum of $\text{UO}_2(\text{FHA})_2$ was also modeled using time dependent-DFT methods. While there has been discussion in the literature of the limitations of TD-DFT for predicting the energies of CT transitions,²¹ the technique can still be used to approximate the spectrum and characterize the transitions.²² The resulting transitions matched reasonably well to the experimental spectrum (Supporting Information Figure S3). The electronic transitions were visualized using natural transition orbitals (NTOs).²³ The two intense transitions at 541 nm and at 553 nm have NTOs that appear as ligand-to-metal charge transfer transitions between the filled π system of the FHA^- ligands and the empty $5f$ orbitals on the uranium. The transition also shows contributions from the uranyl fragment mixed with the ligand π system (Supporting Information Figures S4 and S5). This analysis is in good agreement with work done by Tsushima.²⁴

In conclusion, the red colorations of the solutions and crystals of $\text{UO}_2(\text{FHA})_2$ are caused by two factors. First, there is some orbital mixing of the $5f/6d$ orbitals of uranium with the oxygen atom $2p$ orbitals from the N—O moiety. There is also donation from the filled π orbital of the FHA^- into empty $5f$ orbitals of U(VI). We propose that these two characteristics are responsible for bending the uranyl cation, weakening the $\text{U}=\text{O}$ bonds, and stabilizing the *cis*-uranyl isomer *in silico*. The red coloration is a direct result of these distortions, namely, through a LMCT electronic transition, and is not caused by reduction to U(V). Martin et al. have demonstrated computationally that the *cis*–*trans* isomerization energies can be as low as 18.0 kcal/mol in the gas phase when strong donors are used as equatorial ligands, as in $[\text{UO}_2(\text{OH})_4]^{2-}$.²⁵ We have calculated a *cis*–*trans* isomerization energy of 17.9 kcal/mol in a water solvent field by introducing FHA^- as an equatorial ligand. The effects of this strong equatorial donor on the electronic structure of uranyl are clearly significant.

■ ASSOCIATED CONTENT

Supporting Information

X-ray crystallographic files in CIF format. Additional experimental details, computational details, figures, and spectra. This material is available free of charge via the Internet at <http://pubs.acs.org>.

■ AUTHOR INFORMATION

Corresponding Authors

*E-mail: schelter@sas.upenn.edu.

*E-mail: albrecht-schmitt@chem.fsu.edu.

Notes

The authors declare no competing financial interest.

■ ACKNOWLEDGMENTS

This material is based upon work supported by the U.S. Department of Energy, Office of Science, Office of Basic Energy Sciences, Heavy Elements Chemistry Program, under Award Number DE-FG02-13ER16414. E.J.S. acknowledges the U.S. Department of Energy, Office of Science, Early Career Research Program (DE-SC0006518) for support of this work.

■ REFERENCES

- (1) Iso, S.; Meguro, Y.; Yoshida, Z. *Chem. Lett.* **1995**, *26*, 365–366.
- (2) Paulenova, A.; Tkac, P.; Matteson, B. S. In *American Nuclear Society, 7th International Conference on Advanced Nuclear Fuel Cycles and Systems*; Boise, ID, September 9–13, 2007; Curran Associates, Inc.: New York, 2007.
- (3) Fondeur, F. F.; Rudisill, T. S. *Sep. Sci. Technol.* **2012**, *47*, 2038–2043.
- (4) (a) Andrieux, F. P. L.; Boxall, C.; May, I.; Taylor, R. J. *J. Sol. Chem.* **2008**, *37*, 215–232. (b) May, I.; Taylor, R. J.; Denniss, I. S.; Wallwork, A. L. *Czech. J. Phys.* **1999**, *49*, 597–601. (c) Taylor, R. J.; May, I. *Czech. J. Phys.* **1999**, *49*, 617–621. (d) Taylor, R. J.; May, I.; Wallwork, A. L.; Denniss, I. S.; Hill, N. J.; Galkin, B. Y.; Zilberman, B. Y.; Fedorov, Y. S. *J. Alloys Compd.* **1998**, *271*, 534–537.
- (5) May, I.; Taylor, R. J.; Denniss, I. S.; Brown, G.; Wallwork, A. L.; Hill, N. J.; Rawson, J. M.; Less, R. J. *J. Alloys Compd.* **1998**, *275*–277, 769–772.
- (6) Bean, A. C.; Peper, S. M.; Albrecht-Schmitt, T. E. *Chem. Mater.* **2001**, *13*, 1266–1272.
- (7) (a) Tourneux, J.-C.; Berthet, J.-C.; Cantat, T.; Thuéry, P.; Mézailles, N.; Ephritikhine, M. *J. Am. Chem. Soc.* **2011**, *133*, 6162. (b) Lu, E.; Cooper, O. J.; McMaster, J.; Tuna, F.; McInnes, E. J. L.; Lewis, W.; Blake, A. J.; Liddle, S. T. *Angew. Chem., Int. Ed.* **2014**, *53*, 6696–6700. (c) Sarsfield, M. J.; Helliwell, M.; Collison, D. *Chem. Commun.* **2002**, 2264. (d) Sarsfield, M. J.; Helliwell, M. *J. Am. Chem. Soc.* **2004**, *126*, 1036–1037. (e) Wilkerson, M. P.; Burns, C. J.; Morris, D. E.; Paine, R. T.; Scott, B. L. *Inorg. Chem.* **2002**, *41*, 3110–3120. (f) Bernstein, K. J.; Do-Thanh, C.; Penchhoff, D. A.; Cramer, S. A.; Murdock, C. R.; Lu, Z.; Harrison, R. J.; Camden, J. P.; Jenkins, D. M. *Inorg. Chim. Acta* **2014**, *421*, 374–379. (g) Vlaisavljevich, B.; Galgiardi, L.; Burns, P. C. *J. Am. Chem. Soc.* **2010**, *132*, 14503–14508.
- (8) Duval, P. B.; Burns, C. J.; Clark, D. L.; Morris, D. E.; Scott, B. L.; Thompson, J. D.; Werkema, E. L.; Jia, L.; Anderson, R. A. *Angew. Chem., Int. Ed.* **2001**, *40*, 3357–3361.
- (9) (a) Villiers, C.; Thuéry, P.; Ephritikhine, M. *Angew. Chem., Int. Ed.* **2008**, *47*, 5892–5893. (b) Szigethy, G.; Raymond, K. N. *J. Am. Chem. Soc.* **2011**, *133*, 7942–7956. (c) Arnold, P. L.; Patel, D.; Wilson, C.; Love, J. B. *Nature* **2008**, *451*, 315–317. (d) Brock, A. M.; Cook, D. H.; Fenton, D. E. *J. Inorg. Nucl. Chem.* **1978**, *40*, 1551–1559.
- (10) Andrews, M. B.; Cahill, C. L. *Chem. Rev.* **2013**, *113*, 1121–1136.
- (11) (a) Camp, C.; Autunes, M. A.; Garcia, G.; Ciofini, I.; Santos, I. C.; Pécaut, J.; Almeida, M.; Marçalo, J.; Mazzanti, M. *Chem. Sci.* **2014**, *5*, 841–846. (b) Jilek, R. E.; Spencer, L. P.; Lewis, R. A.; Scott, B. L.; Hayton, T. W.; Boncella, J. M. *J. Am. Chem. Soc.* **2012**, *134*, 9876–9878. (c) Lukens, W. W.; Edelstein, N. M.; Magnani, N.; Hayton, T. W.; Fortier, S.; Seaman, L. A. *J. Am. Chem. Soc.* **2013**, *135*, 10742–10754. (d) Bénéaud, O.; Berthet, J. C.; Thuéry, P.; Ephritikhine, M. *Inorg. Chem.* **2011**, *50*, 12204–12214.
- (12) Oh, G. N.; Ringe, E.; Van Duijne, R. P.; Ibers, J. A. *J. Solid State Chem.* **2012**, *185*, 124–129.
- (13) (a) Kuechle, W.; Dolg, M.; Stoll, H.; Preuss, H. *J. Chem. Phys.* **1994**, *100*, 7535. (b) Cao, X.; Dolg, M.; Stoll, H. *J. Chem. Phys.* **2003**, *118*, 487. (c) Cao, X.; Dolg, M. *THEOCHEM* **2004**, *673*, 203.
- (14) (a) Barone, V.; Cossi, M. *J. Phys. Chem. A* **1998**, *102*, 1995–2001. (b) Cossi, M.; Rega, N.; Scalmani, G.; Barone, V. *J. Comput. Chem.* **2003**, *24*, 669–681.
- (15) Glendening, E. D.; Badenhop, J. K.; Reed, A. E.; Carpenter, J. E.; Bohmann, J. A.; Morales, C. M.; Landis, C. R.; Weinhold, F. *NBO 6.0*; Theoretical Chemistry Institute, University of Wisconsin: Madison, WI, 2013.
- (16) (a) Mayer, I. *Chem. Phys. Lett.* **1983**, *97*, 270. (b) Mayer, I. *Int. J. Quantum Chem.* **1984**, *26*, 151.
- (17) Mullane, K. C.; Lewis, A. J.; Yin, H.; Carroll, P. J.; Schelter, E. J. *Inorg. Chem.* **2014**, *53*, 9129–9139.
- (18) Denning, R. G. *J. Phys. Chem. A* **2007**, *111*, 4125–4143.
- (19) Arnold, P. L.; Pécharman, A.; Hollis, E.; Yahia, A.; Maron, L.; Parsons, S.; Love, J. *Nat. Chem.* **2010**, *2*, 1056–1061.
- (20) Merrick, J. P.; Moran, D.; Radom, L. *J. Phys. Chem. A* **2007**, *111*, 11683.
- (21) Dreuw, A.; Head-Gordon, M. *J. Am. Chem. Soc.* **2004**, *126*, 4007–4016.

- (22) Wiebke, J.; Moritz, A.; Glorius, M.; Moll, H.; Bernhard, G.; Dolg, M. *Inorg. Chem.* **2008**, *47*, 3150–3157.
- (23) Martin, R. L. *J. Chem. Phys.* **2003**, *118*, 4775–4777.
- (24) Tsushima, S. *Dalton Trans.* **2011**, *40*, 6732–6737.
- (25) (a) Clark, D. L.; Conradson, S. D.; Donohoe, R. J.; Keogh, D. W.; Morris, D. E.; Palmer, P. D.; Rogers, R. D.; Tait, C. D. *Inorg. Chem.* **1999**, *38*, 1456–1466. (b) Schreckenbach, G.; Hay, P. J.; Martin, R. L. *Inorg. Chem.* **1998**, *37*, 4442–4451.